A HYBRID GMM/SMC DIFFUSION BERNOULLI FILTER FOR JOINT DISTRIBUTED DETECTION AND TRACKING

Stiven S. Dias

Embraer S.A.
São José dos Campos SP 12227-901, Brazil
+55 12 3927-5428; stiven.dias@embraer.com.br

Marcelo G. S. Bruno

Instituto Tecnológico de Aeronáutica
São José dos Campos SP 12228-900, Brazil
+55 12 3947-6906; bruno@ita.br

ABSTRACT

We introduce in this paper the Random Exchange Diffusion Bernoulli Filter (RndEx-BF), which enables joint target detection and tracking by a network of collaborative sensors. RndEx-BF is a fully distributed algorithm that, unlike consensus-based solutions, does not require iterative internode communication between sensor measurements. Internode communication cost is further reduced by a novel hybrid GMM/SMC implementation of the proposed filter. Experimental results show that RndEx-BF approaches the performance of a flooding-based implementation of the optimal centralized Bernoulli filter with much lower bandwidth requirements.

***Index Terms*—** Bernoulli Filter, Sequential Monte Carlo, Diffusion, RSS Sensors, Joint Detection and Tracking.

1. INTRODUCTION

Fully distributed algorithms for cooperative tracking of hidden state vectors using multiple sensor network observations have been extensively proposed in recent times using both linear Kalman filters, e.g. [1], [2], [3], and particle filters (PFs), e.g. [4], [5], [6], [7], [8]. In more challenging scenarios, however, the tracked state vector may randomly appear in or disappear from the network's surveillance space and the network must perform joint detection and tracking at each time instant.

In [9], we considered the problem of fully distributed detection and tracking in an application of received-signal-strength (RSS) sensor networks by extending the original kinematic state vector with an additional discrete-valued state that indicated presence or absence of the emitter. Distributed particle filtering [10] was then performed in all dimensions of the extended state space. In the present paper, we follow an alternative, more efficient approach based on random finite sets (RFS) and set calculus [11]. Our goal is to derive a new, fully distributed version of the RFS-based Bernoulli filter [12], [13] for joint detection and tracking of a single emitter.

To achieve the desired low internode communication cost requirements, we apply to the Bernoulli filter framework the random exchange diffusion technique in [7] allowing each network node to recursively propagate both its estimated posterior probability of presence of the emitter and the posterior probability density function of the kinematic state vector given that the emitter is present, with both posteriors conditioned on a random subset of network measurements coming from random locations in the entire network. Unlike consensus-based algorithms [4], [5], [6], the proposed algorithm does not require multiple iterative internode communication between the arrival of two consecutive sensor measurements. A novel low-bandwidth approximate implementation of the derived RndEx-BF tracker is additionally proposed combining Gaussian mixture models (GMMs) [14] and sequential Monte Carlo (SMC) methods [15].

The paper is divided into 6 Sections. Sec. 1 is this Introduction. In Sec. 2, we review the models for state dynamics and RSS sensor observations using the RFS formalism. In Sec. 3, we derive the novel distributed RndEx-BF algorithm using set calculus and the methodology in [7]. Sec. 4 describes the hybrid GMM/SMC implementation of the algorithm proposed in Sec. 3. Simulations results, including comparisons to the optimal centralized Bernoulli filter, are presented in Section 5. Finally, we offer our conclusions in Sec. 6.

2. STATE AND SENSOR MODEL

Notation We use uppercase letters, e.g. X_n, to denote random finite sets or samples of random finite sets with the proper interpretation implied in context. Lowercase letters, e.g. $\mathbf{x}_n$, are used to denote both random vectors and samples of random vectors, again with the proper interpretation implied in context[1]. Probability density functions (p.d.f's) of random finite sets, see definition in [11], are denoted by $\tilde{f}(X)$ whereas $f(\mathbf{x})$ denotes the p.d.f. of a random vector. Accordingly, we denote the integral of a set function [11] g as $\int g(X)\,\delta X$ and the integral of a function h of a real variable as $\int h(x)\,dx$. The symbol $\mathcal{N}(m, \sigma^2)$ denotes a one-dimensional Gaussian distribution with mean m and variance σ^2 and the symbol $\propto$ denotes "proportional to".

[1]When a random vector has dimension 1×1, we denote it using lowercase italic letters, e.g. $z_{n,r}$.

Target Model Let $\boldsymbol{S} \subseteq \mathbb{R}^2$ denote a surveillance space in the (x, y) plane. Assuming that at most one target is present in $\boldsymbol{S}$ at any given discrete time instant n, the state *set* at time n is modeled as an RFS [11] whose samples X_n can be either the empty set $X_n = \emptyset$ in case the target is absent, or a single-element set $X_n = \{\mathbf{x}_n\}$, when a single target with state vector $\mathbf{x}_n$ is present. When a target is present, $\mathbf{x}_n = [x_n\, \dot{x}_n\, y_n\, \dot{y}_n]^T$ collects the positions and velocities of the target centroid, respectively in the x and y coordinates.

When no target is present at instant n, a new target may enter the surveillance space $\boldsymbol{S}$ at instant $n+1$ with birth probability p_b. In this case, the initial target state is modeled as a random vector $\mathbf{x}_{n+1}$ distributed according to a prior p.d.f. $f_b(\mathbf{x}_{n+1})$. Conversely, when a single target with state $\mathbf{x}_n$ is present, it stays within $\boldsymbol{S}$ with survival probability $p_v(\mathbf{x}_n)$ or leaves $\boldsymbol{S}$ at instant $n+1$ with probability $1 - p_v(\mathbf{x}_n)$. If the target survives, the state vector at instant $n+1$ given a realization $\mathbf{x}_n$ of the state vector at instant n is modeled by a random vector $\mathbf{x}_{n+1}$ distributed according to the transition p.d.f. $f(\mathbf{x}_{n+1}|\mathbf{x}_n)$.

Given the assumptions in the previous paragraph, the corresponding *set* transition p.d.f. is given by, see [12],

$$\tilde{f}(X_{n+1}|X_n) = \begin{cases} 1 - p_b;\ X_n = \emptyset,\ X_{n+1} = \emptyset \\ p_b\, f_b(\mathbf{x}_{n+1});\ X_n = \emptyset,\ X_{n+1} = \{\mathbf{x}_{n+1}\} \\ 1 - p_v(\mathbf{x}_n);\ X_n = \{\mathbf{x}_n\},\ X_{n+1} = \emptyset \\ p_v(\mathbf{x}_n)\, f(\mathbf{x}_{n+1}|\mathbf{x}_n);\ X_n = \{\mathbf{x}_n\}, \\ \qquad\qquad\qquad\qquad X_{n+1} = \{\mathbf{x}_{n+1}\}. \end{cases} \tag{1}$$

In this paper, we assume the linear white noise acceleration model used in [7] to specify $f(\mathbf{x}_{n+1}|\mathbf{x}_n)$. The survival probability $p_v(\mathbf{x}_n)$ is defined accordingly as the probability of the target staying within $\boldsymbol{S}$ at instant $n+1$ given its current state $\mathbf{x}_n$, i.e. $p_v(\mathbf{x}_n) = Pr(\{\mathbf{x}_{n+1} \in \boldsymbol{S}\}|\mathbf{x}_n) = \int_{\boldsymbol{S}} f(\mathbf{x}|\mathbf{x}_n) d\mathbf{x}$, where $Pr(A)$ denotes the probability of an event A.

Observation Model We assume that each node r in a network of R RSS sensors always records at instant n a single-element RFS measurement taking values $Z_{n,r} = \{z_{n,r}\}$, such that, if $X_n = \{\mathbf{x}_n\}$, then $z_{n,r} \mid \mathbf{x}_n \sim \mathcal{N}(g_r(\mathbf{x}_n), \sigma_r^2)$ with $g_r(.)$ defined as [16]

$$g_r(\mathbf{x}) = P_0 - 10\,\zeta_r \log\left(\frac{\|\mathbf{H}\mathbf{x} - \mathbf{x}_r\|}{d_0}\right), \tag{2}$$

where $\mathbf{x}_r$ is the r-th sensor position, $||.||$ is the Euclidean norm, (P_0, d_0, ζ_r) are known model parameters, see [16], and $\mathbf{H}$ is a 2×4 matrix such that $H(1,1) = H(2,3) = 1$ and $H(i,j) = 0$ otherwise. If, on the other hand, $X_n = \emptyset$, then the sensors record only background noise and $z_{r,n} \sim \mathcal{N}(0, \sigma_r^2)$.

Under the previous assumptions, the set observation p.d.f. at sensor r at instant n is given by [11], [12]

$$\tilde{f}(\{z_{n,r}\}|X_n) = \begin{cases} N_1(z_{n,r} - g_r(\mathbf{x}_n), \sigma_r^2), & X_n = \{\mathbf{x}_n\} \\ N_1(z_{n,r}, \sigma_r^2), & X_n = \emptyset, \end{cases} \tag{3}$$

where $N_L(\mathbf{m}, \mathbf{\Sigma}) = \frac{1}{(2\pi)^{L/2}|\mathbf{\Sigma}|^{1/2}} \exp(-\frac{1}{2}\mathbf{m}^T\mathbf{\Sigma}^{-1}\mathbf{m})$.

3. RANDOM EXCHANGE DIFFUSION BERNOULLI FILTER

Assume that, at instant n, any given node s in the network has a set p.d.f. $\tilde{f}_s(X_n|\mathcal{Z}_{0:n,s})$ where $\mathcal{Z}_{0:n,s}$ collects all RFS observations that have been assimilated by node s from instant 0 up to instant n. We also assume that

$$\tilde{f}_s(X_n|\mathcal{Z}_{0:n,s}) = \begin{cases} 1 - \gamma_{n|n,s}, & X_n = \emptyset \\ \gamma_{n|n,s}\, f_{n|n,s}(\mathbf{x}_n), & X_n = \{\mathbf{x}_n\}, \end{cases} \tag{4}$$

where $\gamma_{n|n,s}$ physically denotes the probability of a target being present in the surveillance space at instant n given the observations contained in the random set $\mathcal{Z}_{0:n,s}$ and $f_{n|n,s}(.)$ denotes the p.d.f. of the state vector $\mathbf{x}_n$ at instant n given that a target is present and given the observations in $\mathcal{Z}_{0:n,s}$. In the sequel, node s sends its set p.d.f. $\tilde{f}_s(X_n|\mathcal{Z}_{0:n,s})$ to a randomly chosen neighboring node r in the vicinity of s and, likewise, receives from node r its corresponding set p.d.f. $\tilde{f}_r(X_n|\mathcal{Z}_{0:n,r})$. Using the set integral version of the total probability theorem [11], and assuming the usual conditional independence hypothesis that $\tilde{f}(X_{n+1}|X_n, \mathcal{Z}_{0:n,s}) = \tilde{f}(X_{n+1}|X_n)$, node r can compute at instant $n+1$, the predicted set p.d.f.

$$\begin{aligned} \tilde{f}_r(X_{n+1}|\mathcal{Z}_{0:n,s}) &= \int \tilde{f}(X_{n+1}|X_n)\, \tilde{f}_s(X_n|\mathcal{Z}_{0:n,s})\, \delta X_n \\ &= \tilde{f}(X_{n+1}|\emptyset)\, \tilde{f}_s(\emptyset|\mathcal{Z}_{0:n,s}) \\ &+ \int \tilde{f}(X_{n+1}|\{\mathbf{x}_n\}) \tilde{f}_s(\{\mathbf{x}_n\}|\mathcal{Z}_{0:n,s})\, d\mathbf{x}_n. \end{aligned}$$

Using (1) and (4), it follows that, for $X_{n+1} = \emptyset$,

$$\begin{aligned} &\tilde{f}_r(\emptyset|\mathcal{Z}_{0:n,s}) = (1 - p_b)\,(1 - \gamma_{n|n,s}) + \gamma_{n|n,s} \\ &\times \int [1 - p_v(\mathbf{x}_n)]\, f_{n|n,s}(\mathbf{x}_n) d\mathbf{x}_n. \end{aligned} \tag{5}$$

Similarly, for $X_{n+1} = \{\mathbf{x}_{n+1}\}$, we get from (1) and (4) that

$$\begin{aligned} &\tilde{f}_r(\{\mathbf{x}_{n+1}\}|\mathcal{Z}_{0:n,s}) = p_b\, f_b(\mathbf{x}_{n+1})(1 - \gamma_{n|n,s}) + \gamma_{n|n,s} \\ &\times \int p_v(\mathbf{x}_n)\, f(\mathbf{x}_{n+1}|\mathbf{x}_n) f_{n|n,s}(\mathbf{x}_n) d\mathbf{x}_n. \end{aligned} \tag{6}$$

Next, solving the system of equations

$$\begin{aligned} 1 - \gamma_{n+1|n,r} &= \tilde{f}_r(\emptyset|\mathcal{Z}_{0:n,s}) \\ \gamma_{n+1|n,r}\, f_{n+1|n,r}(\mathbf{x}_{n+1}) &= \tilde{f}_r(\{\mathbf{x}_{n+1}\}|\mathcal{Z}_{0:n,s}) \end{aligned}$$

with $\tilde{f}_r(\emptyset|\mathcal{Z}_{0:n,s})$ and $\tilde{f}_r(\{\mathbf{x}_{n+1}\}|\mathcal{Z}_{0:n,s})$ given respectively by (5) and (6), it follows after some algebraic manipulation that

$$\gamma_{n+1|n,r} = (1 - \gamma_{n|n,s}) p_b + \gamma_{n|n,s} \int p_v(\mathbf{x}_n)\, f_{n|n,s}(\mathbf{x}_n)\, d\mathbf{x}_n \tag{7}$$

and

$$\begin{aligned} &\gamma_{n+1|n,r}\, f_{n+1|n,r}(\mathbf{x}_{n+1}) = (1 - \gamma_{n|n,s}) p_b\, f_b(\mathbf{x}_{n+1}) \\ &+ \gamma_{n|n,s} \int p_v(\mathbf{x}_n)\, f(\mathbf{x}_{n+1}|\mathbf{x}_n) f_{n|n,s}(\mathbf{x}_n)\, d\mathbf{x}_n. \end{aligned} \tag{8}$$

Let $\mathcal{Z}_{n+1,r}$ denote in the sequel the *disjoint union* of the RFS observation $Z_{n+1,r}$ available at node r at instant $n+1$ and the RFS observations $\{Z_{n+1,l}\}$ available at all nodes $l \in \boldsymbol{N}(r)$, where $\boldsymbol{N}(r)$ denotes the neighborhood of node r. Using the set version of Bayes Law [11], node r at instant $n+1$ computes then the updated conditional set p.d.f. $\tilde{f}_r(X_{n+1}|\mathcal{Z}_{0:n+1,r})$ where $\mathcal{Z}_{0:n+1,r} = \mathcal{Z}_{n+1,r} \cup \mathcal{Z}_{0:n,s}$ by making

$$\tilde{f}_r(X_{n+1}|\mathcal{Z}_{0:n+1,r}) = \frac{\tilde{f}(\mathcal{Z}_{n+1,r}|X_{n+1})}{\tilde{C}_{n+1,r}}\, \tilde{f}_r(X_{n+1}|\mathcal{Z}_{0:n,s}), \tag{9}$$

where the proportionality constant $\tilde{C}_{n+1,r}$ is computed as [11]

$$\tilde{f}(\mathcal{Z}_{n+1,r}|\emptyset)\tilde{f}_r(\emptyset|\mathcal{Z}_{0:n,s}) + \int \Big[\tilde{f}(\mathcal{Z}_{n+1,r}|\{\mathbf{x}_{n+1}\}) \times\, \tilde{f}_r(\{\mathbf{x}_{n+1}\}|\mathcal{Z}_{0:n,s})d\mathbf{x}_{n+1}\Big]. \tag{10}$$

In (9), we used the usual assumption of conditional independence of current and past observations given the current state, i.e $\tilde{f}(\mathcal{Z}_{n+1,r}|X_{n+1},\mathcal{Z}_{0:n,s}) = \tilde{f}(\mathcal{Z}_{n+1,r}|X_{n+1})$. Moreover, provided that the sensor measurement noise is independent from node to node and $\mathcal{Z}_{n+1,r}$ is a disjoint union of $Z_{n+1,r}$ and the sets $Z_{n+1,l}$, $\forall l \in \boldsymbol{N}(r)$, we can write further that

$$\tilde{f}(\mathcal{Z}_{n+1,r}|X_{n+1}) = \prod_{l\in\{r\}\cup\boldsymbol{N}(r)} \tilde{f}(Z_{n+1,l}\,|\,X_{n+1}) \tag{11}$$

with $\tilde{f}(Z_{n+1,l}|X_{n+1})$ given by (3) replacing n with $n+1$. The disjoint union hypothesis is guaranteed if each sensor measurement is uniquely identified by its label, see [11].

Substituting (3) in (11), and (11) in (9), and recalling that $\tilde{f}_r(\emptyset|\mathcal{Z}_{0:n,s}) = 1 - \gamma_{n+1|n,r}$ and $\tilde{f}_r(\{\mathbf{x}_{n+1}\}|\mathcal{Z}_{0:n,s})$ $= \gamma_{n+1|n,r}\ f_{n+1|n,r}(\mathbf{x}_{n+1})$, it follows, after solving for $\tilde{f}_r(\emptyset|\mathcal{Z}_{0:n+1,r}) = 1 - \gamma_{n+1|n+1,r}$ and $\tilde{f}_r(\{x_{n+1}\}|\mathcal{Z}_{0:n+1,r})$ $= \gamma_{n+1|n+1,r}\, f_{n+1|n+1,r}(\mathbf{x}_{n+1})$, that

$$f_{n+1|n+1,r}(\mathbf{x}_{n+1}) = \left[\prod_{l\in\bar{\boldsymbol{N}}(r)} \lambda_{z_{n+1,l}}(\mathbf{x}_{n+1})\right] \frac{f_{n+1|n,r}(\mathbf{x}_{n+1})}{C_{n+1,r}} \tag{12}$$

where $\bar{\boldsymbol{N}}(r) = \{r\} \cup \boldsymbol{N}(r)$, the proportionality constant $C_{n+1,r}$ in (12) is given, at each node r, by the integral

$$C_{n+1,r} = \int \left[\prod_{l\in\bar{\boldsymbol{N}}(r)} \lambda_{z_{n+1,l}}(\mathbf{x}_{n+1})\right] f_{n+1|n,r}(\mathbf{x}_{n+1})\, d\mathbf{x}_{n+1},$$

and

$$\lambda_{z_{n,l}}(\mathbf{x}_n) = \frac{N_1(z_{n,l} - g_l(\mathbf{x}_n), \sigma_l^2)}{N_1(z_{n,l}, \sigma_l^2)} \tag{13}$$

with $N_1(.)$ and $g_l(.)$ defined as in the observation model (3). Similarly, we can also show that

$$\gamma_{n+1|n+1,r} = \frac{\gamma_{n+1|n,r}\, C_{n+1,r}}{(1-\gamma_{n+1|n,r}) + \gamma_{n+1|n,r}\, C_{n+1,r}}. \tag{14}$$

4. HYBRID GMM/SMC IMPLEMENTATION

In this Section, we introduce an approximate implementation of the diffusion Bernoulli filter derived in Sec. 3. Assume that node s at instant n has a weighted particle set $\{(w_{n,s}^{(j)}, \mathbf{x}_{n,s}^{(j)})\}$, $j \in \{1, 2, \ldots, J_b + J\}$, which represents the p.d.f. $f_{n|n,s}(\mathbf{x}_n)$ in the Monte Carlo sense [15]. We fit that Monte Carlo representation then to a GMM [14] to build a parametric approximation to $f_{n|n,s}$ given by

$$\hat{f}_{n|n,s}(\mathbf{x}_n) = \sum_{k=1}^{\mathcal{K}} \eta_{n,s}^{(k)}\, N_L(\mathbf{x}_n - \mathbf{m}_{n,s}^{(k)},\, \boldsymbol{\Sigma}_{n,s}^{(k)}), \tag{15}$$

where $L = 4$. In addition, using the weighted particle set, the integral on the right-hand side of (7), which is the expected value of $p_v(\mathbf{x}_n)$ with respect to the p.d.f. $f_{n|n,s}(\mathbf{x}_n)$, is approximated locally at node s as $\hat{p}_{v,s} = \sum_{j=1}^{J_b+J} w_{n,s}^{(j)}\, p_v(\mathbf{x}_{n,s}^{(j)})$.

Node s now transmits to the neighboring node r only the parameters of the GMM approximation in (15) plus $\gamma_{n|n,s}$ and $\hat{p}_{v,s}$. Node r then performs the calculations in (7) and (8) replacing $f_{n|n,s}$ with $\hat{f}_{n|n,s}$ and $p_v(\mathbf{x}_n)$ with $\hat{p}_{v,s}$. Eq. (7) thus reduces to $\gamma_{n+1|n,r} = (1-\gamma_{n|n,s})p_b + \hat{p}_{v,s}\gamma_{n|n,s}$. Assuming further as in [7] that $\mathbf{x}_{n+1}|\mathbf{x}_n \sim \mathcal{N}(\mathbf{F}\,\mathbf{x}_n, \mathbf{Q})$, the integral on the right-hand side of (8) is in turn computed analytically[2] as

$$\hat{I}(\mathbf{x}_{n+1}) = \sum_{k=1}^{\mathcal{K}} \hat{p}_{v,s}\eta_{n,s}^{(k)} N_L(\mathbf{x}_{n+1} - \mathbf{F}\mathbf{m}_{n,s}^{(k)}, \mathbf{F}\boldsymbol{\Sigma}_{n,s}^{(k)}\mathbf{F}^T + \mathbf{Q}).$$

In the sequel, node r samples at instant $n+1$ a new set of particles $\mathbf{x}_{n+1,r}^{(j)} \sim f_b(\mathbf{x}_{n+1})$, $j = 1, \ldots, J_b$ and $\mathbf{x}_{n+1,r}^{(j)} \sim \hat{I}(\mathbf{x}_{n+1})/\hat{p}_{v,s}$, $j = J_b+1, \ldots, J_b+J$. From (8) and (12), it can be shown that $\{(w_{n+1,r}^{(j)}, \mathbf{x}_{n+1,r}^{(j)})\}$, $j \in \{1, \ldots, J_b+J\}$, is a properly weighted particle set to represent $f_{n+1|n+1,r}(\mathbf{x}_{n+1})$ at node r at instant $n+1$ provided that

$$w_{n+1,r}^{(j)} \propto \tilde{w}_{n+1|n,r}^{(j)} \prod_{l\in\{r\}\cup\boldsymbol{N}(r)} \lambda_{z_{n+1,l}}(\mathbf{x}_{n+1.r}^{(j)}) \tag{16}$$

with proportionality constant such that $\sum_j w_{n+1,r}^{(j)} = 1$ and

$$\tilde{w}_{n+1|n,r}^{(j)} = \begin{cases} \frac{(1-\gamma_{n|n,s})p_b}{J_b\gamma_{n+1|n,r}} & j = 1, \ldots, J_b. \\ \frac{\gamma_{n|n,s}\hat{p}_{v,s}}{J\,\gamma_{n+1|n,r}} & j = J_b+1, \ldots, J_b+J. \end{cases} \tag{17}$$

Finally, $\gamma_{n+1|n+1,r}$ is updated at node r according to (14) using the approximation

$$C_{n+1,r} \approx \sum_{j=1}^{J_b+J} \tilde{w}_{n+1|n.r}^{(j)} \prod_{i\in\{r\}\cup\boldsymbol{N}(r)} \lambda_{z_{n+1,l}}(\mathbf{x}_{n+1.r}^{(j)}). \tag{18}$$

If $\gamma_{n+1|n+1,r} > 1/2$, node r decides that the target is present at instant $n+1$ and estimates its kinematic state as $\hat{x}_{n+1|n+1,r}$ $= \sum_j w_{n+1,r}^{(j)}\, \mathbf{x}_{n+1,r}^{(j)}$ with $j \in \{1, \ldots, J_b+J\}$.

[2]The closed form solution to the integral in (8) is restricted to linear, Gaussian dynamic models. On the other hand, provided that one is able to compute the likelihood ratios in (13), the proposed implementation can be used with arbitrary non-linear, possibly non-Gaussian observation models.

5. SIMULATION RESULTS

We evaluated the performance of the RndEx-BF tracker over 100 Monte Carlo runs in a simulated scenario with $R = 25$ RSS sensors scattered within a surveillance space $\boldsymbol{S}$ of size $120\,\text{m} \times 120\,\text{m}$. The sensor model parameters were kept fixed during all Monte Carlo runs and set to the same values as in [9]. Fig. 1 shows the sensor positions, the available network connections assuming that each node communicates with other nodes within a range of $40\,\text{m}$, and two consecutive realizations of the emitter trajectory within a simulation period of $200\,\text{s}$.

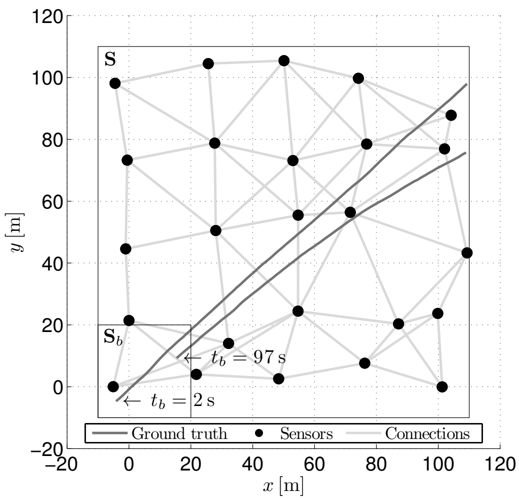

Fig. 1. Evaluated scenario.

The prior set p.d.f. $\tilde{f}_s(X_0)$ at each node s was initialized at time step 0 with a priori probability of target presence $\gamma_{0|0,s} = 0$. The birth density $f_b(\mathbf{x}_{n+1})$ was assumed uniform on a square $\boldsymbol{S}_b \subset \boldsymbol{S}$ of size $30\,\text{m} \times 30\,\text{m}$ for the emitter's initial position in Cartesian coordinates and Gaussian with mean $\left[\sqrt{2}\,\text{m/s} \quad 45°\right]^T$ and covariance matrix $diag(0.3^2, 5^2)$ for the emitter's initial velocity in polar coordinates.

The RndEx-BF tracker using a single Gaussian[3], i.e. $\mathcal{K} = 1$, was compared to the ReDif-PF tracker proposed in [9] and to an alternative flooding [17] implementation of the optimal centralized Bernoulli filter [12], referred to in this paper as the CbBF tracker. Each node r running the CbBF tracker assimilates its local measurement $Z_{n+1,r}$ only and uses then the flooding scheme in [8] to compute, in a fully distributed fashion, the joint likelihood of all network measurements at time $n+1$. The RndEx-BF and CbBF trackers employed $J_b = J = 250$ particles to represent the posterior $f_{n|n,s}(\mathbf{x}_n)$ at a node s. To avoid unnecessary computations, when $\gamma_{n|n,s} \approx 0$, both algorithms sampled J_b particles from the prior $f_b(\mathbf{x}_{n+1})$ only. Most of the time though, when $\gamma_{n|n,s} \approx 1$, they sampled just J particles from the proposal $\hat{I}(\mathbf{x}_{n+1})/\hat{p}_{v,s}$. The ReDif-PF tracker, on the other hand, employed a fixed number of 500 particles along all simulated emitter trajectories.

Fig. 2 shows the root-mean-square (RMS) error norm of the emitter position estimates over time for the evaluated algorithms. The RMS error was computed considering all simulated emitter trajectories at each Monte Carlo run. The bars along the curves represent the standard deviation of the error norm across all network nodes. As expected, compared to CbBF, which mimics the optimal centralized Bernoulli filter, the RndEx-BF tracker has a greater RMS error since it assimilates less information at each network location than the former. On the other hand, despite using a lower number of particles throughout most of the emitter trajectory, RndEx-BF has a much lower RMS error compared to ReDif-PF, especially after the second emitter is acquired, indicating that RndEx-BF is not significantly affected by the on/off switching of the emitter presence/absence state as ReDif-PF is.

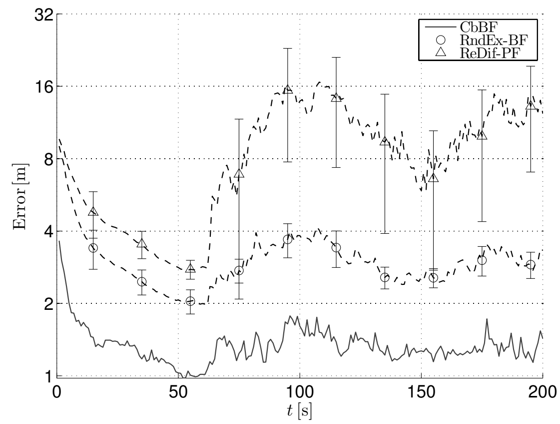

Fig. 2. Evolution of the estimated position RMS error norm.

Table 1 summarizes the communication and computation cost of each algorithm, see [9] for a description of the performance metrics. The RndEx-BF tracker has an average communication cost per node three orders of magnitude lower than that of the CbBF with one sixth of the processing cost. The global probability of error (misses or false alarms) over all network node detection decisions was $0.02\,\%$ for the RndEx-BF detector, down from $0.22\,\%$ when ReDif-PF was used. No detection errors were made by CbBF in our experiments.

Table 1. Average communication and processing cost.

	RX Rate	**TX Rate**	**Duty Cycle**
CbBF	116 KB/s	24 KB/s	7.6 %
ReDif-PF	148 B/s	132 B/s	2.9 %
RndEx-BF	156 B/s	140 B/s	1.3 %

6. CONCLUSIONS

We introduced in this paper the RndEx-BF filter for joint target detection and tracking in sensor networks. RndEx-BF is a fully distributed algorithm that does not require iterative internode communication between sensor measurements. Communication cost is further reduced using a novel hybrid GMM/SMC implementation of the filter. Experimental results show that RndEx-BF approaches the performance of the optimal CbBF algorithm, but with lower communication cost, and also compares favorably to the joint detector/tracker proposed in [9].

[3] No significant improvement was observed for $\mathcal{K} = 2$.

7. REFERENCES

[1] F. S. Cattivelli, and A. H. Sayed, "Diffusion strategies for distributed Kalman filtering and smoothing," *IEEE Transactions on Automatic Control*, vol. 55, no. 9, pp. 2069–2084, September 2010.

[2] I. D. Schizas, G. B. Giannakis, S. I. Roumeliotis, and A. Ribeiro, "Consensus in Ad Hoc WSNs with noisy links-Part II: distributed estimation and smoothing of random signals," *IEEE Transactions on Signal Processing*, vol. 56, no. 4, pp. 1650–1666, April 2008.

[3] S. Kar and J. M. F. Moura, "Gossip and distributed Kalman filtering: weak consensus under weak detectability," *IEEE Transactions on Signal Processing*, vol. 59, no. 4, pp. 1766–1784, April 2011.

[4] O. Hlinka, O. Sluciak, F. Hlawatsch, P. Djuric, and M. Rupp, "Likelihood consensus and its applications to distributed particle filtering," *IEEE Transactions on Signal Processing*, vol. 60, no. 8, pp. 4334–4349, August 2012.

[5] A. Mohammadi and A. Asif, "Consensus-based distributed unscented particle filter," *2011 IEEE Statistical Signal Processing Workshop*, pp. 237–240, Nice, France, June 2011.

[6] D. Uztebay, M. Coates, and M. Rabat, "Distributed auxiliary particle filter using selective gossip," *IEEE Intl. Conf. on Acoustics Speech and Sig. Proc.*, pp. 3296–3299, Prague, Czech Republic, May 2011.

[7] M. G. S. Bruno and S. S. Dias, "Cooperative emitter tracking using Rao-Blackwellized random exchange diffusion particle filters," *Eurasip Journal on Advances in Signal Processing*, 2014:19, pp. 1–18, February 2014, doi: 10.1186/1687-6180-2014-19.

[8] S. S. Dias and M. G. S. Bruno, "Cooperative target tracking using decentralized particle filtering and RSS sensors," *IEEE Transactions on Signal Processing*, vol. 61, no. 14, pp. 3632–3646, July 2013.

[9] S. S. Dias and M. G. S. Bruno, "Joint Emitter Detection and Tracking using Distributed Random Exchange Diffusion Particle Filtering," *Proc. IEEE Intl. Conf. on Acoustics, Speech, and Sig. Proc.*, Florence, Italy, May 2014.

[10] O. Hlinka, F. Hlawatsch, and P. M. Djuric, "Distributed Particle Filtering in Agent Networks: A Survey, Classification, and Comparison," *IEEE Signal Processing Magazine*, vol. 30, no. 1, pp. 61–81, January 2013.

[11] R. Mahler, "*Statistical Multisource Multitarget Information Fusion*, Norwood, MA, USA: Artech House, 2007.

[12] B. Ristic, B.-T. Vo , B.-N. Vo, and A. Farina, " A tutorial on Bernoulli filters: theory, implementation and applications," *IEEE Transactions on Signal Processing*, vol.61, no. 13, pp. 3406 - 3430 , July 2013.

[13] B.-T. Vo, D. Clark, B.-N. Vo, and B. Ristic, "Bernoulli Forward-Backward Smoothing for Joint Target Detection and Tracking," *IEEE Transactions on Signal Processing*, vol. 59, n. 9, pp. 4473-4477, September 2011.

[14] X. Sheng, Y. H. Hu, and P. Ramanathan, "Distributed particle filter with GMM approximation for multiple targets localization and tracking in wireless sensor network," in *Proc. IPSN*, pp. 181–188, Los Angeles CA, U.S.A., April 2005.

[15] A. Doucet, S. J. Godsill, and C. Andrieu, "On sequential Monte Carlo sampling methods for Bayesian filtering," *Statistics and Computing*, vol. 10, no. 3, pp. 197–208, 2000.

[16] N. Patwari, A. O. Hero III, M. Perkins, N. S. Correal, and R. J. O'Dea, "Relative location estimation in wireless sensor networks," *IEEE Transactions on Signal Processing*, vol. 51, n. 3, pp. 2137-2148, March 2003.

[17] D. Tsoumakos and N. Roussoupoulos, "A comparison of peer-to-peer search methods," in *Proceedings of the WebDB*, pp. 61–66, San Diego CA, June 2003.